A Predictive PBM-DEAM Model for Lignocellulosic Biomass Pyrolysis

Hongyu Zhu[1], Zhujun Dong[2], Xi Yu [1,*], Grace Cunningham[1], Janaki Umashanker[1], Xingguang Zhang[3], Anthony V. Bridgwater[1], Junmeng Cai [2,*]

[1] Energy & Bioproducts Research Institute (EBRI), College of Engineering and Physical Sciences, Aston University, Aston Triangle, Birmingham B4 7ET, United Kingdom

[2] Biomass Energy Engineering Research Center, Key Laboratory of Urban Agriculture (South) Ministry of Agriculture, School of Agriculture and Biology, Shanghai Jiao Tong University, 800 Dongchuan Road, Shanghai 200240, People's Republic of China

[3]Department of Chemistry, School of Science, University of Shanghai for Science and Technology, 516 Jungong Road, Shanghai 200093, PR China

* Corresponding authors: Xi Yu, x.yu3@aston.ac.uk; Junmeng Cai, jmcai@sjtu.edu.cn

Highlights:

- PBM-DAEM coupled model is first time developed to predict biomass pyrolysis.
- Population balance model is used to present the feedstock size distribution.
- Non-isothermal kinetics without and with DEAM capture the intra-particle temperature distribution.
- Noticeable difference of heating-up time between single and distributed particle size is observed.

Graphic abstract

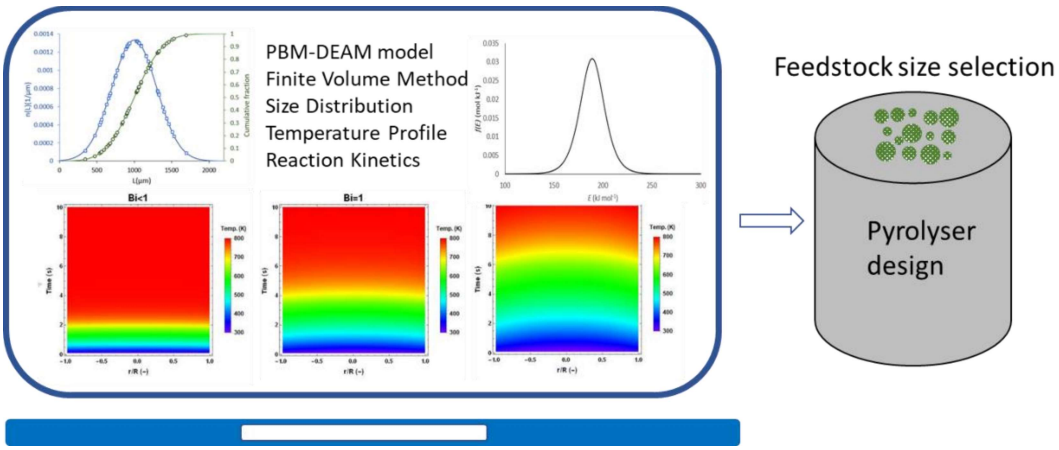

Abstract

Pyrolysis is a promising and attractive way to convert lignocellulosic biomass into low carbon-emission energy products. To effectively use biomass feedstock with size distribution to produce biofuels, a comprehensive kinetic model of the process, occurring at particle level, is important. In this study, the population balance model (PBM)-distributed activation energy model (DAEM) coupled model is first time developed to predict biomass pyrolysis. The Population balance model is used to present the variable size distribution of solid, decomposed from virgin biomass to porous char. Two different kinetic models are embedded into the conservation equations of mass and energy. They are compared to demonstrate the prediction performance of heating-up time during the pyrolysis process of biomass with a normal size distribution. It is found that non-isothermal kinetics without and with DEAM capture the intra-particle temperature distribution. There is a noticeable difference of heating-up time between single and distributed particle size.

Key words: Distributed activation energy model (DAEM); Population balance model (PBM); Kinetics; Biomass pyrolysis; Temperature distribution

Nomenclature

Abbreviations

CFD	Computational fluid dynamics
DAEM	Distributed activation energy model
PBM	Population balance model
M	Moisture content
VM	Volatile matter
FC	Fixed carbon
PHLEFR	Plasma heated laminar entrained flow reactor
SFOR	Single first order reaction

Roman symbols

A	Pre-exponential factor in Arrhenius expression
Bi	Biot number
Cp	Heat capacity
E	Activation energy
H	Reaction heat
h	External heat transfer coefficient
k	Kinetic constant

k_{eff}	Effective thermal conductivity of biomass
L	Characteristic length
N	Division number of the finite volume approach
$\tilde{Q}$	Reaction heat absorbed by solid remains
R	Universal gas constant
r	Particle radius
$\dot{r}$	Conversion rate
T	Temperature
t	Time
V	Volume
X	Mass fraction

Greek symbols

ρ	Bulk density
ρ_0	Initial density of biomass particle
μ	Mean value
σ	Standard deviation
α	Conversion degree
ω	Pore emissivity

Subscripts

B	Biomass
c	Core of the biomass particle
dev	Devolatilization process
dry	Drying process
M	Moisture
V	Volatile
C	Char
p	Particle
s	Surface of the biomass particle
0	Initial value

Superscripts

db	Dry biomass

1. Introduction

The pyrolysis is a thermochemical conversion process which converts organic materials into liquid, solid and gases, occurring in the absence of oxygen [1]. The yields of the solid, liquid and gases

production from pyrolysis largely depend on the operation conditions [2], reactor configuration [3] and physicochemical properties of biomass [4]. The fast pyrolysis technology for liquid products has been developed in recent decades [5]. It can produce high yields of liquid fuel (up to 75 wt%) at moderate operation temperature and short residence times (less than 2s) [6]. Fast pyrolysis technology also can be used to recover energy from different types of waste, e.g. municipal solid waste [7], sewage sludge [8], oily sludge [9] and plastics [10]. The fast pyrolysis represents the rapid heating-up rate, short vapours residence time, fast cooling down rate and high bio-oil yield [11]. As the liquid products have higher energy density than solid or gas fuels and they are easy to be transported and used, the fast pyrolysis of biomass currently attracts great attention in the field of energy [5]. The reaction path of the biomass pyrolysis is complex, including the primary decomposition of the biomass components, the secondary cracking stage and the re-polymerization process [12].

In order to gain the maximum liquid production yield in fast pyrolysis of biomass, several features must to be characterized in the process [5, 13]: the operation temperature need to be controlled precisely around 500 ^{o}C; the moisture content within the biomass feedstock to reactor is less than 10%; the particle size of biomass after pre-treatment is typically less than (e.g. 3mm for fluidised bed) to get high heating-up rate; the rapid removal rate and high removal efficiency of char and fast vapours cooling rate are needed to minimize the thermal cracking. The particle size is one of the most important design parameters in fast pyrolysis of biomass. Bennadji et al. [14] investigated the effect of particle sizes on the processing time and the product yield and found that the required heating and devolatilization time increased as the particle size increasing. The heat penetration into biomass particles occurs from the surface, then transfer into the particle core by heat conduction [12]. Thus, the appropriate particle sizes will be a prerequisite to ensure a rapid heating rate during biomass fast pyrolysis.

As particle size primarily determines the heating up of biomass and its decomposition progress in biomass pyrolysis, a mathematical model to predict heat up time of bulk biomass is desirable but relevant literature is lack. One exceptional candidate is the population balance approach, which is applied to the particulate materials modelling process, describing the properties evolution of a group of particles with varying sizes as the function of time and position [15]. The population balance equations were firstly presented by Hulburt and Katz [16] in 1964, calculating the particle size distribution of the dispersed phase. Since then, the Population Balance Model (PBM) has been popularly introduced to particles in process modelling (e.g., the granulation [17-19] and crystallization [20] processes), to investigate the way of change in biomass particle size distribution. Basic mechanisms of the PBM for evolution of the particle size distribution are: nucleation, growth, aggregation and breakage [21]. In the thermochemical conversion, the change in the biomass particle size results from the particle volume shrinkage and char breakage behaviours [22, 23].

A comprehensive understanding of the biomass pyrolysis kinetics plays an important role in investigating mass and heat transfer mechanism, which contributes to a more accurate model for reactor

design and process optimization when coupled with CFD simulation [24-27]. Many kinetic models have been proposed to describe biomass pyrolysis kinetics. The single first order reaction (SFOR) model has been used widely due to its simplicity, however, it is an empirical model limited to a single reaction with a single activation energy [28]. Currently, the state-of-the-art model applied to describe the thermal decomposition kinetics of solid fuels is the distributed activation energy model (DAEM) [25, 29-32]. It has been used to analyse the thermal decomposition kinetics of solid fuels, including biomass and its lignocellulosic components, coal, oil shale, waste plastics, and polymer etc. [32]. The model assumes that biomass pyrolysis takes a large number of independent parallel first-order or *n*th-order reactions with their own activation energies reflecting variations in the bond strengths of biomass species [29] and that the difference in activation energy can be described by a continuous distribution function (e.g., Gaussian, Logistic, Weibull distribution functions) [33, 34].

The ultimate objective of this work is to develop a model framework, which can simulate the pyrolysis process of biomass with a size distribution by predicting (1) real time intra-particle temperature distribution, which update volume averaged temperature of non-isothermal kinetics model at each time step; (2) heating up time of biomass particles with a size distribution, which is helpful for the design of pyrolysis reactors and determination of optimal feedstock particle sizes.

2. Model descriptions

In this study, a particle level model framework coupled with PBM and DEAM is developed to: (1) simulate the intra-particle pyrolysis process, and (2) predict heating-up time of feedstock with a size distribution. The particle level model is primarily comprised of mass conservation and energy conservation equations, which are comprehensively described in section 2.1. Figure 1 shows the algorithm of PBM-DEAM coupled model. Model input requires particle size distribution, boundary conditions (e.g. particle temperature, pyrolysis temperature and particle density) and kinetic parameters. By using the kinetic parameters, the mass loss at each time step is calculated via DEAM. The partial differential equations of the particle heat and mass transfer are discretized and solved via finite volume method. The profile of particle temperature and mass are updated and recorded.

PBM is used to present particle size distribution by sampling a finite number of feedstocks. The detail of PBM is described in section 2.2. Two different kinetics models (Non-isothermal with DEAM and without DAEM) are coupled into mass conservation equations to characterize the chemical reaction kinetics of biomass pyrolysis. The pyrolysis kinetics with DEAM for biomass pyrolysis is described in section 2.3. The numerical calculations are carried out in the Wolfram Mathematica software system. The finite volume approach is used to solve the energy conservation equation relating the intra-particle heat transfer. Finite volume approach has two major advantages: (a) The flux (e.g. mass, momentum,

energy) entering a given volume is identical to that leaving the adjacent volume, these methods are conservative; (b) it is easily formulated to allow for unstructured meshes to approximate complex geometries [35].

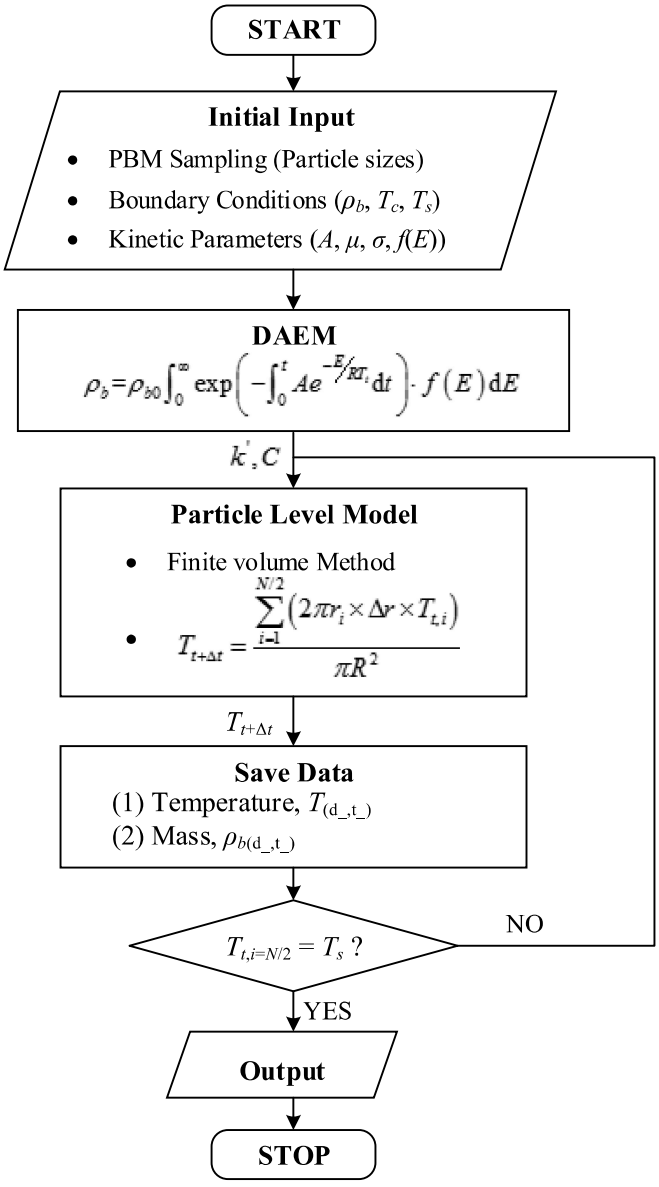

Figure 1: Algorithm of PBM-DEAM coupled model.

In this work, the modelled biomass feedstock was peach wood and the proximate analysis and the ultimate analysis of the peach branch were presented in *Table 1.*

Table 1: Proximate analysis and the ultimate analysis of the biomass material.

Proximate analysis				
Moisture	**Volatile**	**Fixed carbon**		**Ash**
8.17 wt.%	79.22 wt.%	10.59 wt.%		2.02 wt.%
Ultimate analysis				
$\mathbf{C^{(db)}}$	$\mathbf{H^{(db)}}$	$\mathbf{O^{(db)}}$	$\mathbf{N^{(db)}}$	$\mathbf{S^{(db)}}$
49.51 wt.%	5.94 wt.%	41.89 wt.%	0.30 wt.%	0.16 wt.%

2.1. Mass and energy conservation

The governing equations of the mathematical model are consisted of the conservation of mass and energy. The ash of biomass particle is assumed to be constant during pyrolysis process. Li et al. [36] presented the equations to describe the mass evolution of biomass components. The mass evolution equations in this model includes the dry biomass (Eq. 1), moisture content (Eq. 2), volatile (Eq.3) and char (Eq.4). In the devolatilisation process, the reaction form is considered as:Biomass → volatiles + char. Thus, the evolution of volatile and char content can be given by the fraction of column.

$$\frac{\partial \mathrm{m}_B}{\partial \mathrm{t}} = -k_{dev}\mathrm{m}_B \tag{1}$$

$$\frac{\partial \mathrm{m}_{moi}}{\partial t} = -k_{dry}\mathrm{m}_{moi} \tag{2}$$

$$\mathrm{m_v} = v_{vola}(\mathrm{m}_{B0} - \mathrm{m}_B) \tag{3}$$

$$\mathrm{m_c} = v_{char}(\mathrm{m}_{B0} - \mathrm{m}_B) \tag{4}$$

where m_B, m_{moi}, $\mathrm{m_v}$, and $\mathrm{m_c}$ are the mass of the dry biomass, moisture, volatile and char. The superscript 0 means the initial value of each column. At *t=0*, $\mathrm{m}_{B0} = \rho_B \mathrm{V}_{P0}(1-\varphi_0)$, the φ_0 is the initial porosity of the particle. The conversion rate is assumed as the first order Arrhenius equation.

The energy conservation of the solid particles is expressed by considering the heat conduction, radiation and heat release during the conversion. The energy conservation equation is described in Eq.5.

$$(1-\varphi)\rho_B C_{P(B)}\frac{\partial T_P}{\partial \mathrm{t}} = \frac{1}{r^2}\frac{\partial}{\partial r}\left(r^2 k_{\mathrm{eff}}\frac{\partial T_P}{\partial r}\right) + \sum \dot{r}_i \Delta H_i + \tilde{Q} \tag{5}$$

where *r* is the radius direction of the particle, $\dot{r}_i$ represents the conversion rate (*i*=M, V, C representing the moisture, volatile and carbon, respectively). The initial and boundary conditions for the above equations are

At $t = 0, T_p = 298\mathrm{K}$

At $r = 0, \frac{\partial T_P}{\partial \mathrm{r}} = 0$

At $r = R, \frac{\partial T_P}{\partial \mathrm{r}} = k_{\mathrm{eff}} \frac{\partial T_P}{\partial r} - \omega\sigma\left(T_{env}^4 - T_p^4\right)$

The effective thermal heat transfer coefficient is described as Eq. 6 [37].

$$k_{\mathrm{eff}} = \eta \times k_B + (1-\eta) \times k_C + \varphi \times k_V + 13.5\sigma T_p^3 l_{pore}/\omega \quad (6)$$

where η = m_B/m_{B0}, which is the ratio of the current biomass mass to the initial mass. The parameter φ is the local porosity of the biomass particle, which is related to the drying and devolatilisation processes [38]. It varies as a linear relationship with the conversion process.

$$\varphi = \varphi_0 + (1-\varphi_0)[\alpha_M(X_{M0} - X_M) + \alpha_V(X_{V0} - X_V) + \alpha_C(X_{C0} - X_C)] \quad (7)$$

where α_M, α_V and α_C are the dimensionless parameter of the particle shrinkage during each conversion processes. X_M, X_V and X_C are the mass fraction at time *t*. The particle volume varies during the conversion processes are considered from the total mass conservation, which means the final particle volume can be solved from the final residue biomass mass.

$$V_P = \frac{(1-\varphi_0)\rho_{B0}V_{P0} - \Delta m_B}{(1-\varphi)\rho_B} \quad (8)$$

The values of the related variables in these equations are given in Table 2 ***Error! Reference source not found.***.

Table 2: Properties and kinetic data.

Properties used in model						
	ρ_B	Density	700	kg m^{-3}		[39]
	X_{M0}	Moisture content (M)	8.17	wt.%		
	X_{V0}	Volatile matter (VM)	79.22	wt.%		
	X_{C0}	Fixed carbon (FC)	10.59	wt.%		
	X_A	Ash	2.020	wt.%		
	v_{vola}	VM/(1- M)	0.862	-		
	v_{char}	FC/(1- M)	0.115	-		
	$C_{p(B)}$	Heat Capacity of biomass	1112 + 4.85×(T_p-273)	J kg^{-1} K^{-1}		[40]
	$C_{p(V)}$	Heat Capacity of volatile	1050 + 0.18×(T_p-273)	J kg^{-1} K^{-1}		
	$C_{p(C)}$	Heat Capacity of char	1390 + 0.36×(T_p-273)	J kg^{-1} K^{-1}		[41]
	$C_{p(M)}$	Heat Capacity of moisture	4280	J kg^{-1} K^{-1}		
Kinetic parameters for devolatilisation						
	A	Pre-exponential factor	1.1291×10^{16}	s^{-1}		
	E	Activation energy	189.15	kJ mol^{-1}		
Kinetic parameters for drying						
	A	Pre-exponential factor	6×10^5	s^{-1}		[42]
	E	Activation energy	48.22	kJ mol^{-1}		[42]
Thermal properties						
	k_M	Thermal conductivity (moisture)	0.653	w m^{-1} K^{-1}		[38, 43]
	k_V	Thermal conductivity (volatile)	0.2	w m^{-1} K^{-1}		[38]

	k_C	Thermal conductivity (char)	0.15	w m^{-1} K^{-1}		[38]
	k_A	Thermal conductivity (ash)	0.1	w m^{-1} K^{-1}		[38]
	k_B	Thermal conductivity (biomass)	0.21	w m^{-1} K^{-1}		[44]
	ΔH_m	Reaction heat (moisture)	-270	kJ kg^{-1}		[37, 45]
	ΔH_v	Reaction heat (volatile)	-418	kJ kg^{-1}		[37]
	ΔH_c	Reaction heat (char)	-418	kJ kg^{-1}		[37]
Other values						
	ω	Pore emissivity	1	-		[43]
	l_{pore}	Pore size	5×10^{-5}	m		[38]
	σ	Stefan-Boltzmann constant	5.67×10^{-8}	w m^{-2} K^{-4}		[46]

Previous studies to explore the differences between the non-isothermal model and the isothermal model are available in the literature [47-49]. The isothermal model neglected the intra-particle heat transfer of biomass particles [50]. The isothermal model showed a reasonable pyrolysis behaviour for small biomass particles (Biot number < 1), while for large particles (Bi > 1), the isothermal model predicted a shorter reaction time compared with the thermally-thick model [51]. Thus, the non-isothermal particle model can be considered to give more accurate simulation results than the isothermal model.

In this study, two different kinetic models for biomass pyrolysis are considered (*Table 3*): (1) Non-isothermal model with DAEM; (2) Non-isothermal model with Arrhenius model.

Table 3: Three simulation conditions.

Case No	Models	Kinetics equations and temperature
1	Non-isothermal with DAEM	DAEM (Equation 9-14) & averaged temperature
2	Non-isothermal without DEAM	First-order Arrhenius kinetics &Averaged temperature

The kinetics parameters following the first-order Arrhenius kinetics are listed in Table 2 **Error! Reference source not found.**, where R is the universal gas constant (8.3145 J K^{-1} mol^{-1}). T_p is the heating temperature of the biomass particle. For non-isothermal model, T_p uses volume averaging method cross the particle every time step. Figure 2 shows the discretization of energy equation (Eq.5) in radial direction for intra-particle heat transfer, and volume averaged temperature is estimated to update thermal properties. The initial conditions of the samples are at 298 K and 1 atm, and it is assumed

that the particles exposed to the heating source at time 0.

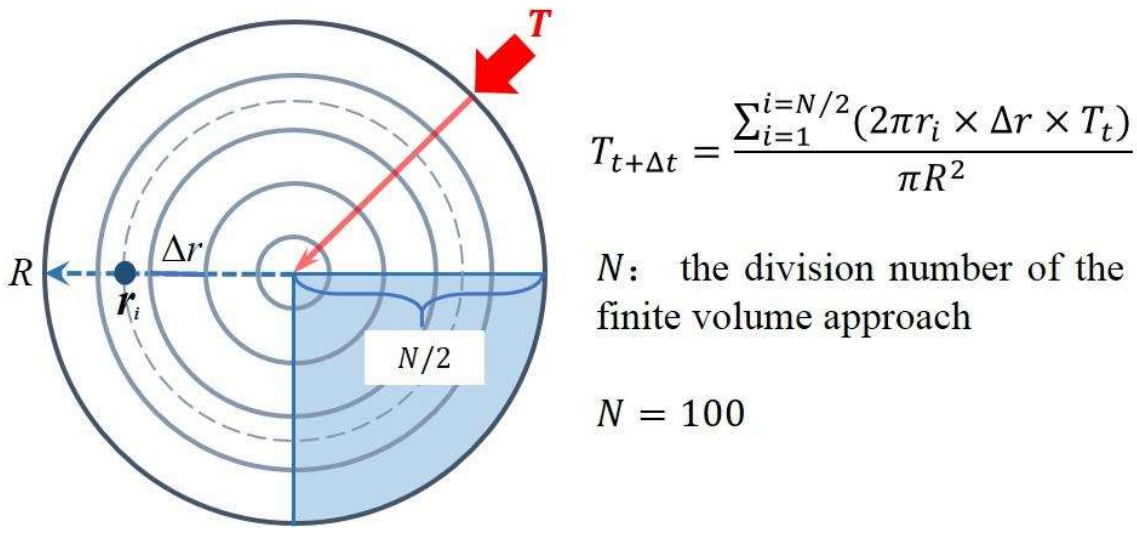

Figure 2: Schematic of intra-particle heat transfer, and average temperature calculation in non-isothermal kinetics model.

The primary assumptions made in this model are listed as follows: (1) the particle has a spherical shape; (2) the external heat convection to the particle surface is not involved, only the external heat radiation and intraparticle heat conduction is considered; (3) the thermal conductivity of the biomass particle is assumed as a constant (although it may change with the char formation).

2.2. Population balance model

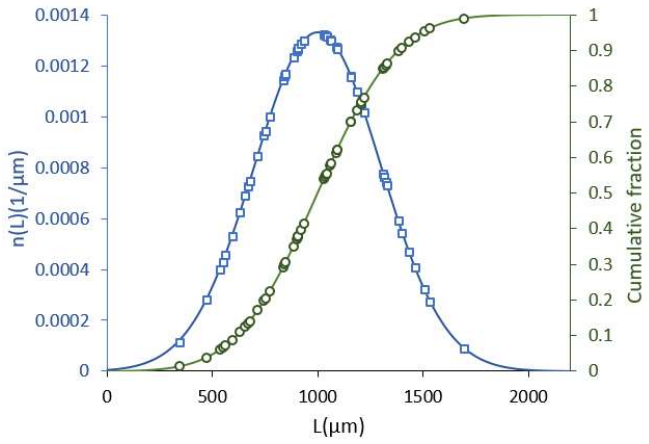

Figure 3 Particle size sampling from a normal distribution (μ_p=1000μm, σ_p=200)

Figure 3 shows particle size sampling from a normal distribution with mean particle size, μ_p= 1000 μm and standard deviation, σ_p = 200 μm. The lines represent the continuous probability of selecting a particle of a given size. The discrete 50 points represent the particles which were randomly selected

from the distribution using the Monte Carlo method. In stochastic method to solve the equations of population balance, the sample number of PSD influences accuracy and computational cost when the number of particles changes with process time. The increase of sample number improves the prediction accuracy while increasing computational cost in the process of particle growth by coalescence [52]. In this study, the number of particles remain constant, thus the appropriate sample number is used to balance accuracy and computational cost.

The Biot number (defined by Eq. 9) is a dimensionless number which describes the ratio of internal heat resistance of a body (which occurs through conduction) to the external heat resistance of a body (which occurs through convection).

$$Bi = \frac{h\,L_p}{k'} \qquad (9)$$

where h is the external heat transfer co-efficient, k' is the thermal conductivity, and L_p is the characteristic length of the particle. As the heat transfer coefficient has not been considered in this model, assumed values for the heat transfer coefficient and thermal conductivity have been used in calculating the Biot number. The thermal properties were assumed as: h= 650 W/m^2 K and k' =0.25 W/m K [53]. Figure 4 shows the relationship between Biot number and particle size to be able to convert between the two values if necessary. It should be noted that, in a real process, the relationship between the Biot number and particle size is not linear as the heat transfer coefficient of biomass is affected by particle size.

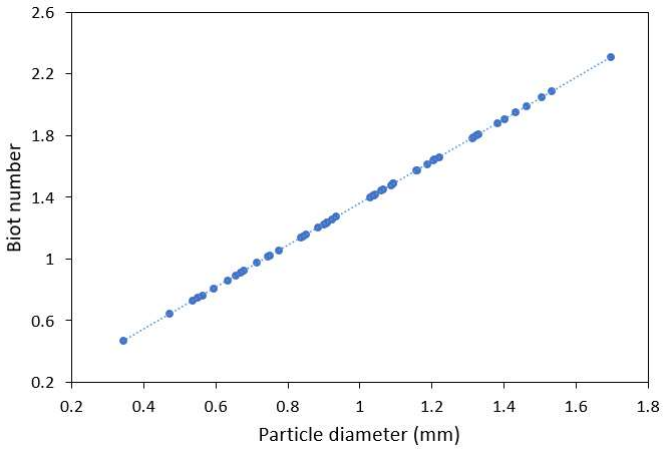

Figure 4: Biot number against particle diameter.

2.3. DEAM model

The DAEM equation can be derived based on the following assumptions: (1) the thermal decomposition of biomass involves a large number of independent and parallel first order reactions; (2) each reaction has its own activation energy and all reactions share the same frequency factor; (3) the activation

energies of all reactions can be described by a continuous distribution [29, 54-56]. With these assumptions, the general form of the DAEM equation can be obtained [29]:

$$\alpha(t) = \int_0^{+\infty} \left\{ 1 - \exp\left[-\int_0^t A\exp\left(-\frac{E}{RT}\right) \mathrm{d}t \right] \right\} f(E)\mathrm{d}E \qquad (10)$$

$$\frac{\mathrm{d}\alpha}{\mathrm{d}t}(t) = \int_0^{+\infty} A\exp\left[-\frac{E}{RT} - \int_0^t A\exp\left(-\frac{E}{RT}\right) \mathrm{d}t \right] f(E)\mathrm{d}E \qquad (11)$$

where α is conversion degree (dimensionless), A is the frequency factor (s^{-1}), E is the activation energy (J mol^{-1}), t is the time (s), T is the temperature (K), and $f(E)$ is the activation energy distribution (mol J^{-1}). The Logistic activation energy distribution is considered in this work because of its advantages in the representation of the kinetics of lignocellulosic biomass pyrolysis (Figure 5) [56].

$$f(E) = \frac{\pi}{\sqrt{3}\sigma} \frac{\exp\left[-\frac{\pi(E-\mu)}{\sqrt{3}\sigma}\right]}{\left\{1+\exp\left[-\frac{\pi(E-\mu)}{\sqrt{3}\sigma}\right]\right\}^2} \qquad (12)$$

where μ is the mean value (J mol^{-1}) and σ is the standard deviation (J mol^{-1}) of the activation energy distribution.

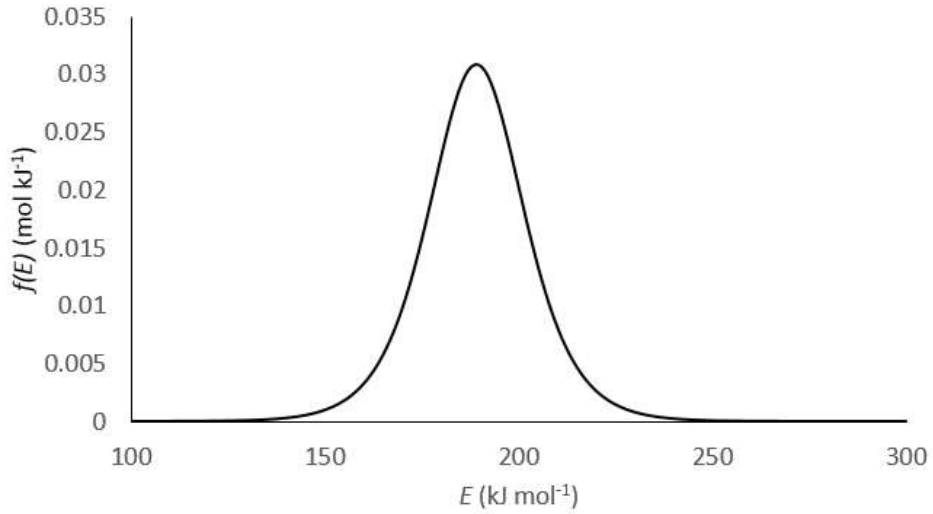

Figure 5: Activation energy distribution for biomass pyrolysis (μ = 189.15 kJ mol-1 and σ = 14.73 kJ mol-1)

For coupling DAEM and PBM, the mass transfer of biomass and conversion rate can be obtained:

$$\alpha = 1 - \frac{\rho}{\rho_0} \qquad (13)$$

$$\frac{\mathrm{d}\alpha}{\mathrm{d}t}(t) = \frac{\mathrm{d}\left(1-\frac{\rho}{\rho_0}\right)}{\mathrm{d}t}(t) = -\frac{1}{\rho_0}\frac{\mathrm{d}\rho}{\mathrm{d}t}(t) \qquad (14)$$

$$\frac{\mathrm{d}\rho}{\mathrm{d}t}(t) = -\rho_0 \int_0^{+\infty} A\exp\left[-\frac{E}{RT} - \int_0^t A\exp\left(-\frac{E}{RT}\right)\mathrm{d}t\right] f(E)\mathrm{d}E \qquad (15)$$

where ρ is the density of biomass particle at time t, and ρ_0 is the initial density of biomass particle.

3. Results and discussion

3.1. Model validation

The developed model framework is firstly validated with a comparison of the numerical results (surface temperature, mass loss and size reduction) to corresponding experimental data obtained from pyrolysis of spherical wood particles [42]. The experiment was carried out by Huang et al. [42], utilising a fixed-bed reactor integrating a high-transparency quartz tube with an electrically heated furnace to study the pyrolysis behaviour of wood particle in spherical shape. The surface temperature of woody biomass in Figure 6 displays the comparison between the experimental data and the model predictions. It is clear that the trend of the numerical predictions (from non-isothermal model without DEAM and with DEAM model) are consistent with the experimental data at 150~400 s, meanwhile a bit over-prediction can be observed before 150 s. The increase of surface temperature is predominantly controlled by boundary conditions, consisting of convective and radiative heat transfer from surrounding pyrolysis environment. The mass loss shown in Figure 7 demonstrates the pyrolysis characteristics, with the weight loss mainly happened at 150 to 250 s, corresponding to surface temperature at 700–750K. The numerical curve of mass loss largely fits the experimental data, with a slight over-prediction of decomposition speed.

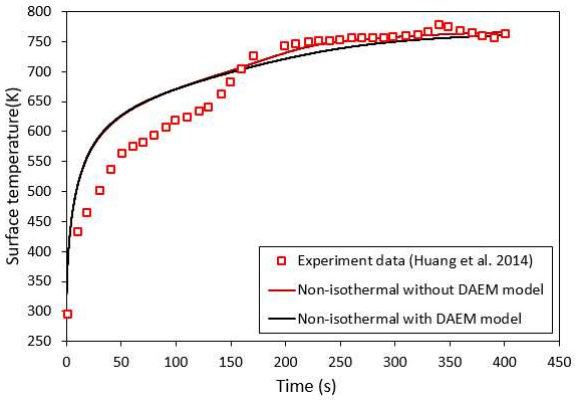

Figure 6: Particle surface temperature. Experiment data obtained from [42].(d=20mm, 773K).

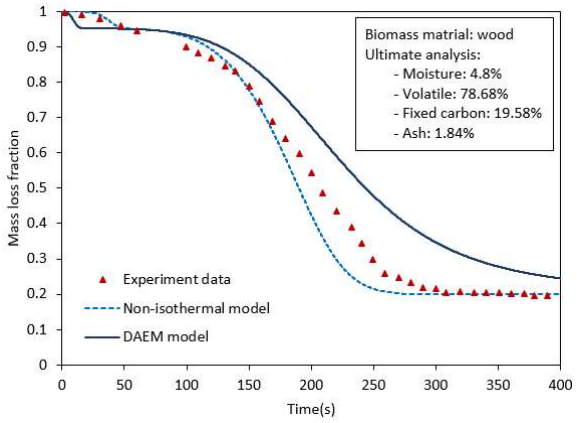

Figure 7: Residue mass fraction (d=20mm, 773K). Experimental data from Huang et al. [42]. Ultimate analysis data obtained from Sadhukhan et al.[57].

Shrinkage percentage is a ratio of instantaneous diameter to initial diameter of the wood sphere. There is no uniform standard of shrinkage model in the literature. Contradictive experimental phenomena were also found that, wood pellets shrinkage increases with temperature in the range 300–1000 °C [58] , whereas wood spheres shrinkage decreases with temperature in the range of 673 to 973K [42]. Two shrinkage models were incorporated into the model framework to simulate the size reduction of wood sphere with 20mm during pyrolysis at 773K. As shown in Figure 8, the shrinkage model developed by Huang et al. [42] using a mathematical function based on Boltzmann fitting, agrees the experimental data fairly well, as the case specific parameters are directly regressed from investigational data size reduction. The shrinkage model developed by Yang et al. [38] is based on mass balance, which could directly apply to this validation with successful prediction of final size, but the accuracy of temporal size reduction is less than the shrinkage model of Huang et al.

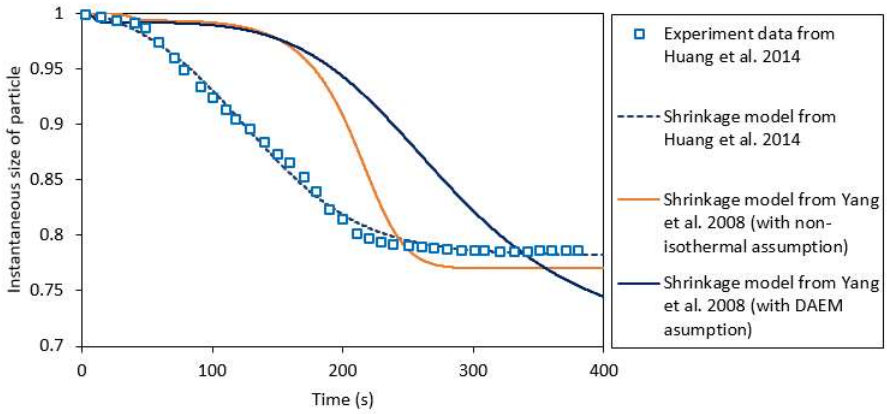

Figure 8: Size reduction comparison. Shrinkage model from: Huang et al. [42] and Yang et al. [38].

3.2. Mass losses

From Section 3.2 to Section 3.5, different kinetics models are utilised to simulate the fast pyrolysis of peach wood with a normal size distribution (in Fig. 3). From the perspective of mathematical modelling, the heat, mass and kinetic transfer phenomenon occur simultaneously in the thermochemical conversion

process of lignocellulosic biomass [59]. Once the particle exposed to the heating source, the biomass particle is heated up and the temperature transferred from the surface. In the heating process, the biomass particle is decomposed while producing volatiles and char, at the same time, the moisture content within the particle is vaporized in a short time period [60]. The mass loss rate of the pyrolysis stage strongly depends on the temperature distribution inside the biomass particles [59].

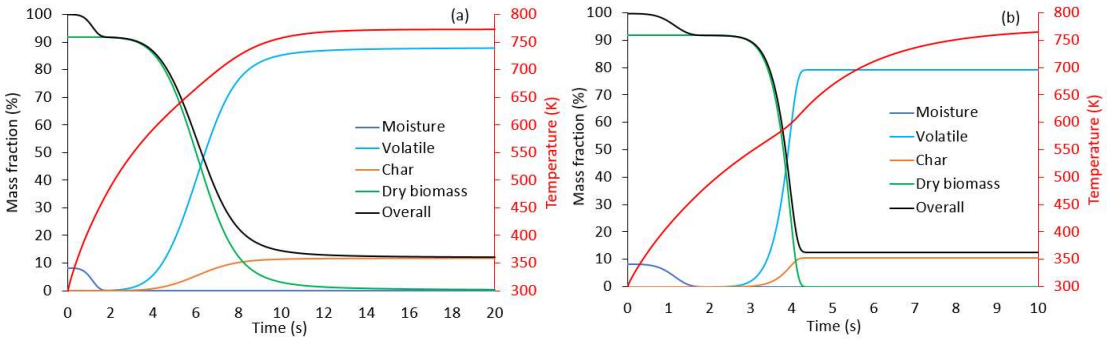

Figure 9: Mass loss rate predicted (d=1.03mm, 773K): (a) Non-isothermal model with DAEM; (b) Non-isothermal model without DAEM.

Figure 9 presents the individual mass change prediction of 1.03 mm spherical biomass particle, which refers the progress of drying and devolatilization known as the two main stages occurred during biomass fast pyrolysis. Therefore, the rate of mass change reflects the accuracy and capture ability of the different models. The drying process terminates quickly less than 2s in the numerical prediction of both non-isothermal models, and predicted high devolatilization rate of non-isothermal model with DEAM appears at 4~8 seconds, which is relatively delayed compared to that of non-isothermal model with DEAM .

DAEM predicted the mass loss rate in function of environment temperature (450~600 ºC) is shown in Figure 10***Error! Reference source not found.***. The increase of environment temperature accelerates thermal degradation of peach wood. Influence of temperature on mass loss rate predicted from non-isothermal model with DAEM (1.03mm). Figure 11 shows the extent of size reduction at different time periods for whole particle population.

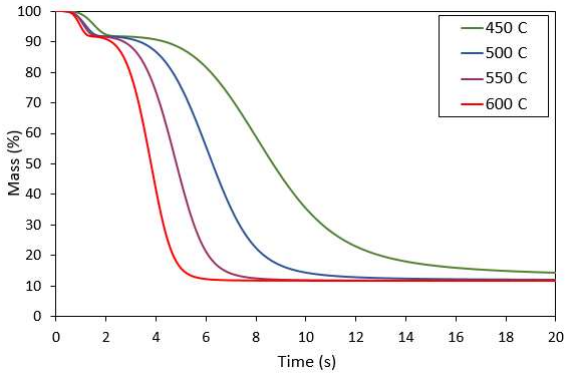

Figure 10: Influence of temperature on mass loss rate predicted from non-isothermal model with DAEM (1.03mm).

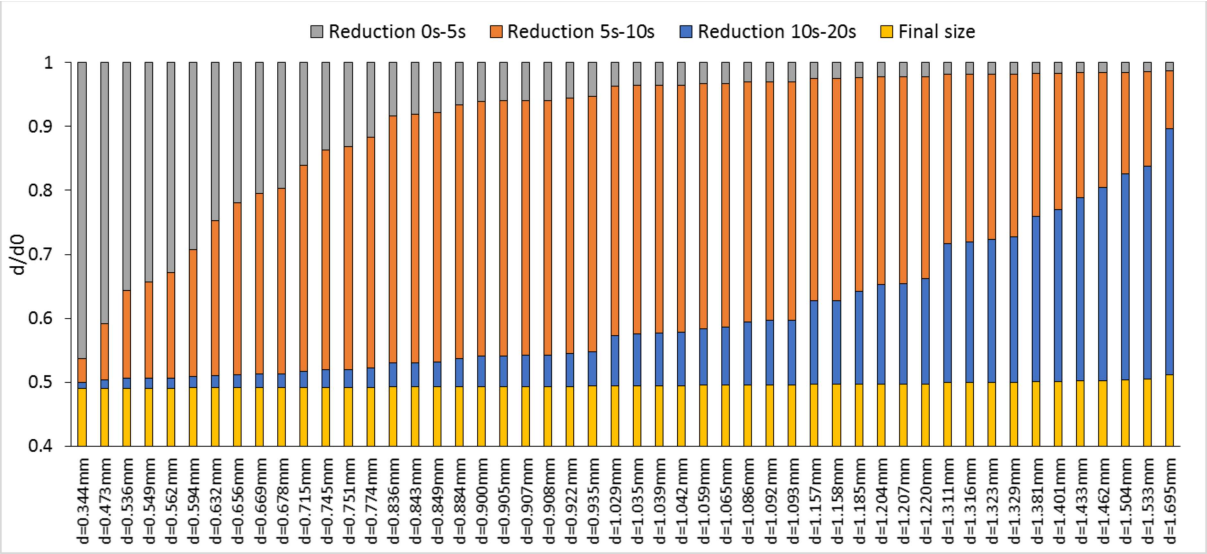

Figure 11: the extent of size reduction at different time periods for whole particle population (non-isothermal model with DAEM)

3.3. Intra-particle temperature distribution, size reduction and porosity

Error! Reference source not found. shows contour plot of radial temperature distribution over time at different Biot number. Fine particle with Bi <1 have achieved uniform temperature cross radial direction over the whole process. There is slight difference between core temperature and surface temperature of wood particle with Bi=1. At Bi >1, the radial temperature distribution within particle is symmetrical and parabolic. The heating up time increases with particle size.

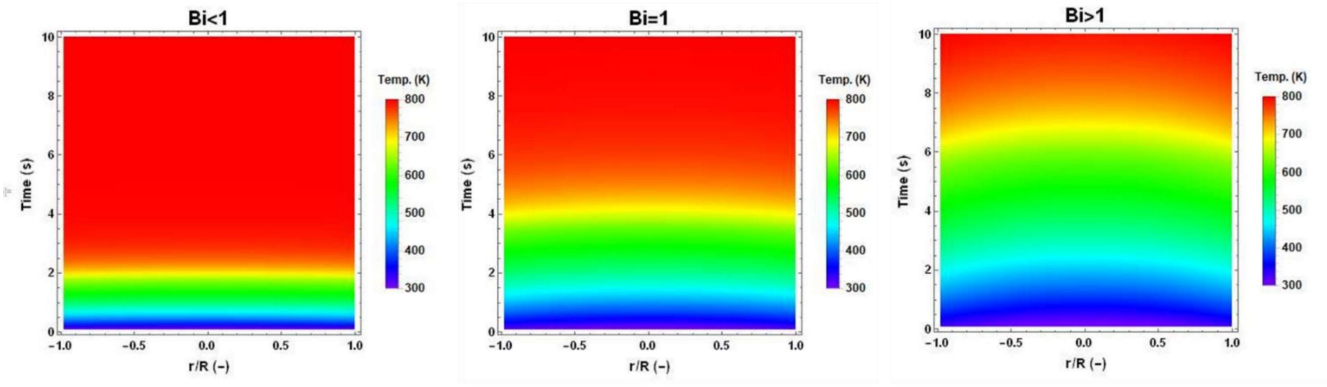

Figure 12: Contour plot of radial temperature distribution over time at different Biot number: d=0.59mm (Bi<1), d=0.74mm (Bi=1), d=1.31mm (Bi>1) by Non-isothermal model with DAEM

The variation of the pore structure within particles might be another reason for the low mass loss rate when shrinkage is tiny. Figure 13 shows the porosity and size reduction over time under two different kinetic models, respectively. It could be observed that rapid increase of porosity synchronize with rapid decrease of the wood mass as the increase of pore size could benefit the releasing rate of gas and tar.

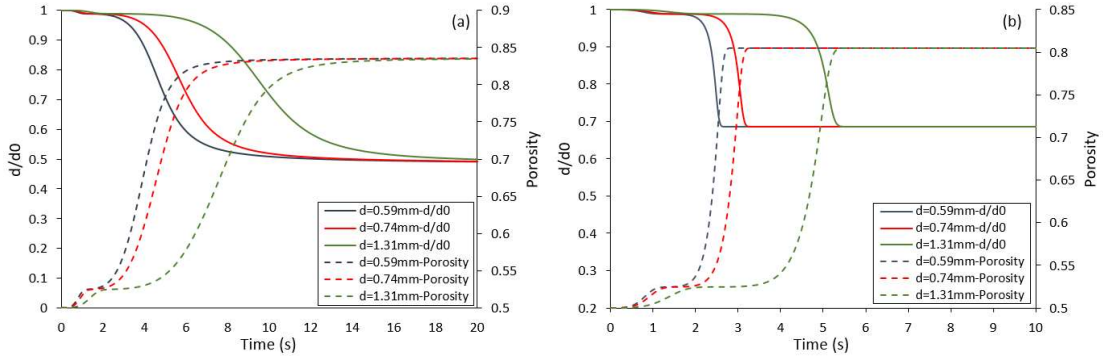

Figure 13: Particle diameter and porosity variation for different particles: d=0.59mm (Bi<1), d=0.74mm (Bi=1), d=1.31mm (Bi>1) at 773K. (a)Non-isothermal with DAEM. (b) Non-isothermal model without DEAM.

3.4. Population level performance

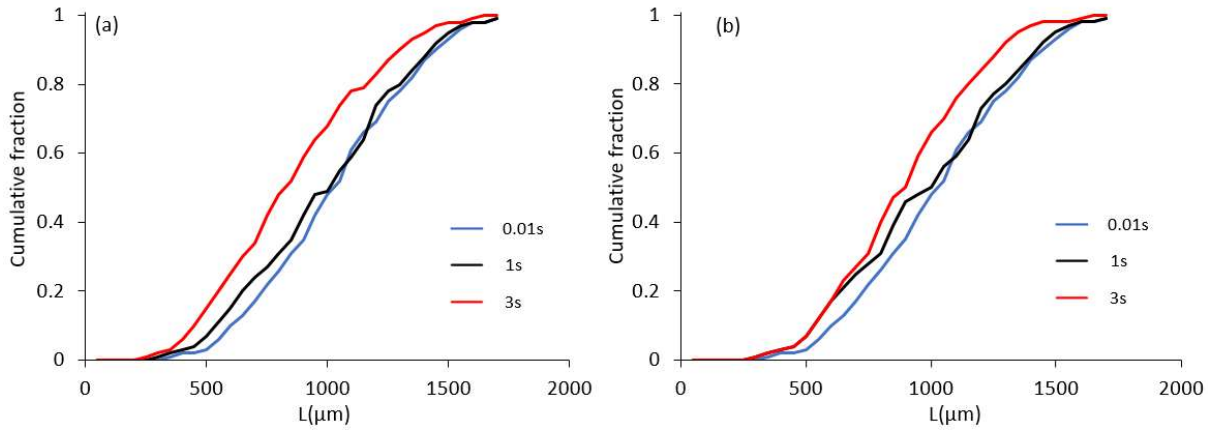

Figure 14: Temporal evolution of particle size distribution at 773K. (a)Non-isothermal with DAEM. (b) Non-isothermal model without DEAM.

Particle shrinkage of biomass leads to temporal evolution of particle size distribution, which is predicted and shown in Figure 14. The partially left shift of cumulative curve of population size distribution at 1 s in Figure 14 shows relatively smaller particles completed the decomposition and size reduction. The overall left shift of cumulative curve population size distribution at 3 s in Figure 14 demonstrates most particles completed the decomposition and size reduction.

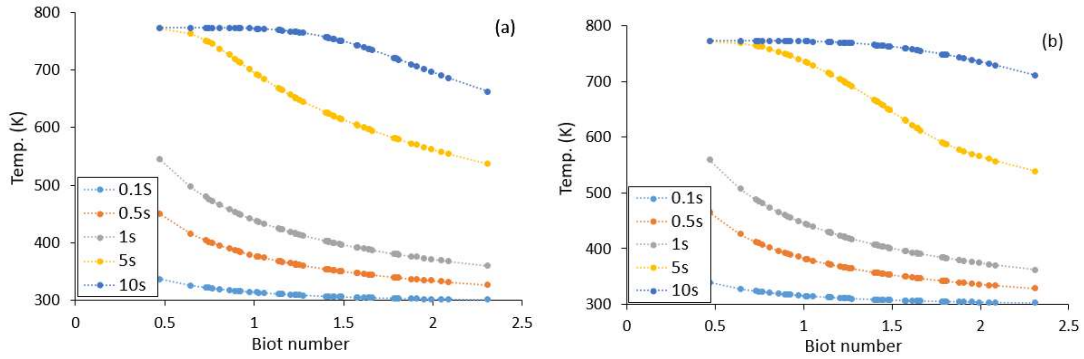

Figure 15: Temperature at particle core at pyrolysis temperature of 773K. (a)Non-isothermal with DAEM. (b) Non-isothermal model without DEAM.

Error! Reference source not found. Figure 15 shows the temperature of particle core, T_c, for particle population (presented as Bi number) at different times. There is always a decrease in T_c with increasing particle size. At 1 s, the smallest particle (Bi = 0.47) has achieved a temperature 545K, whilst T_c of the largest particle (Bi = 2.3) is only at 360K. The initial heating rate of the smallest particle indicated rapid heating up occurring at fine particles in fast pyrolysis processes, which well agreed with the experimental observation**.** Furthermore, all particles with Bi <1 have achieved some extent of increase in temperature after just 0.1 s, with T_c decreasing as Biot number increases up. At Bi >1, T_c has not increased significantly from its initial temperature, and does not appear to be affected by particle size above Bi>1. This builds upon the idea that the critical Biot number is Bi=1 ([61], [62] and [63]), as above Bi=1, there is evidence that the heat transfer resistance of the particle has prevented T_c from being significantly increased. After 10 s, we see that T_c of particles with a Bi up to 1.2 have achieved the temperature of the surroundings, 773K. Above Bi=1.2, there is again a decline in T_c with increasing particle size. Figure 16 shows high pyrolysis temperature advantages heat transfer through the particle.

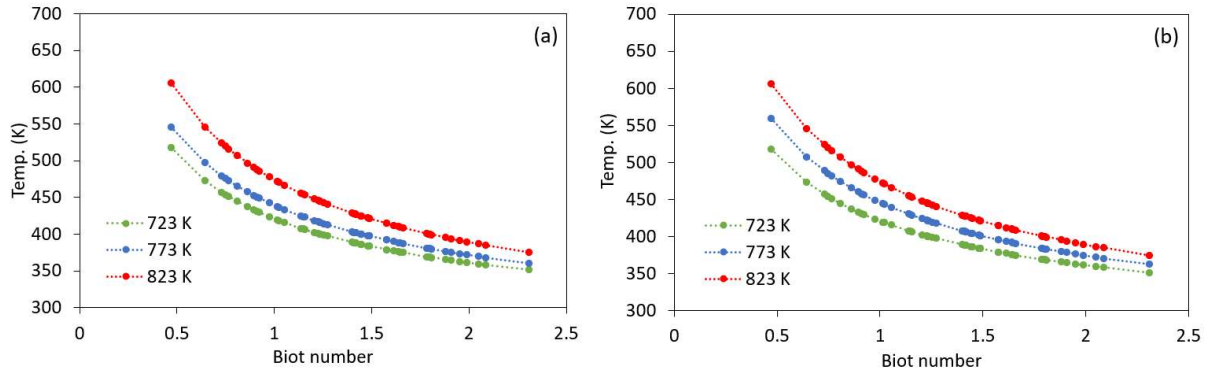

Figure 16: Effect of pyrolysis temperature on temperature of particle core after 1 Second. (a)Non-isothermal with DAEM. (b) Non-isothermal model without DEAM.

Figure 17 demonstrates the capability of PBM to predict the temporal percentage of particle population to complete heating up process. The PBM model enables proper particle size of biomass feedstock to be selected for satisfying the affirmatory resident time distribution of pre-installed reactor. In Figure 17 (a), the numerical prediction of pyrolysis at 723K indicates that only 38% of particles have undergone complete heating-up process after 10 s. It takes 17.2 s for all of the particles in the size distribution to complete heating-up process. At 823K, we see that a significantly higher proportion of the particles have achieved complete thermal transfer after 10s, around 98%.

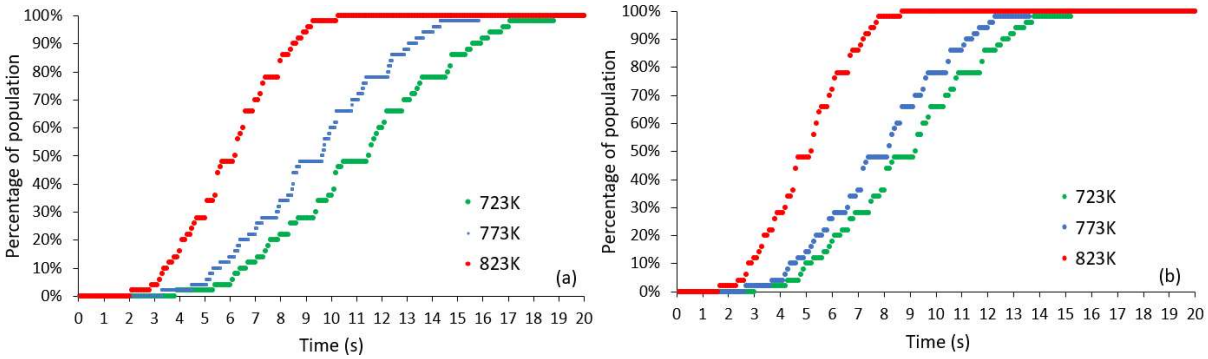

Figure 17: Percentage of PSD to complete heating up process predicted from different models under temperature. (a)Non-isothermal with DAEM. (b) Non-isothermal model without DEAM.

3.5. Heating-up time of normal size distribution

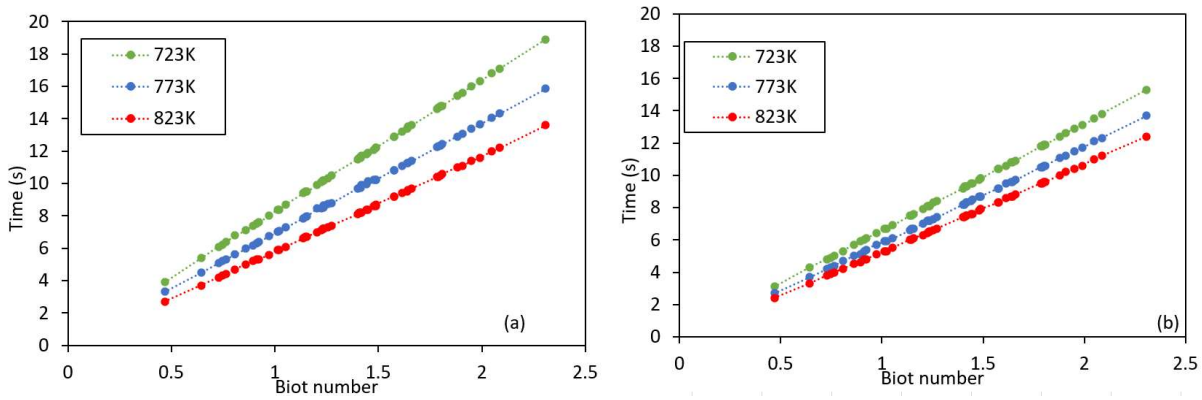

Figure 18: Heat up time under different surrounding temperature. (a)Non-isothermal with DAEM. (b)Non-isothermal model.

Figure 18 shows the dependence of heat-up time on the size of particle at different pyrolysis temperature of 723K~823K. As the particle diameter increases, so does the time taken for T_c to achieve surrounding temperature, which is in agreement with results reported in the literature [64]. For both non-isothermal kinetic models, the increase of exposure temperature accelerates heating up of biomass feedstock, especially for thermally thick particle.

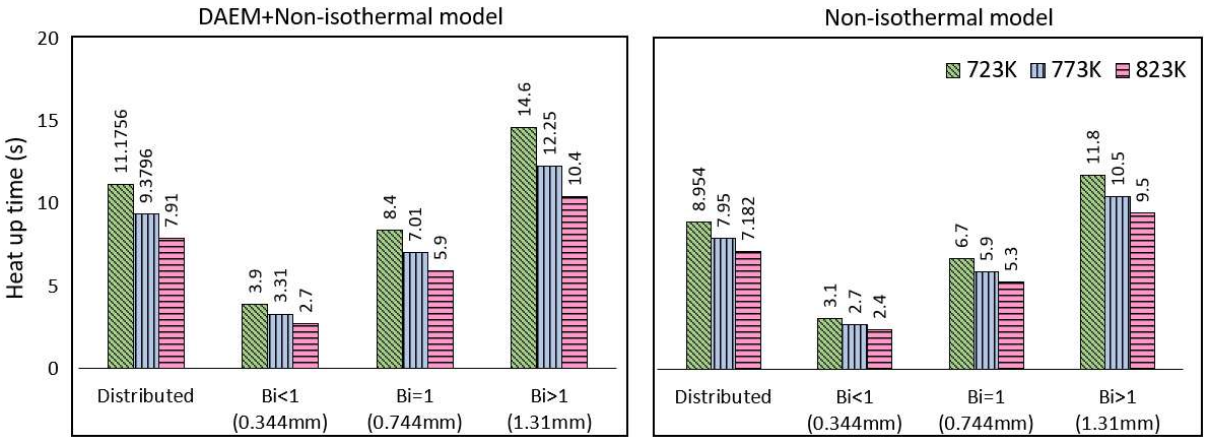

Figure 19: Comparison of heating up time prediction between single and distributed particle size using different kinetics models.

Figure 19 shows the comparison of heating-up time between single and distributed particle size using different kinetics models. The order of predicted heating up time is: Non-isothermal without DEAM < Non-isothermal with DEAM. The heating up time of normal size distribution is always larger compared to that of single size for all three models. For non-isothermal model with DEAM, the heat-up time for single size of 1mm in is found to be 11.1 and 9.0 s, respectively. This is in good agreement with the work of Wiggins, et al. [65], who found the time taken for the surface of a 1mm spherical particle to reach 773K to be 3 seconds. Figure 20 shows the comparison of heating-up time between single and distributed particle size under different surrounding temperatures.

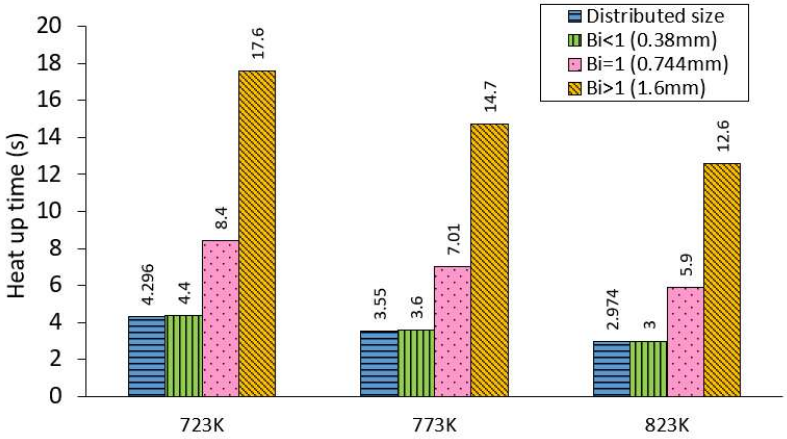

Figure 20: Comparison of heating up time prediction between single and distributed particle size under different temperature.

3.6. Heating up time of irregular size distribution

In section 3.4, the results undoubtedly indicate that there is a noticeable difference of heating-up time between single and distributed particle size. In this section, we aim to explore the effect of particle size distribution on heating-up time prediction. Figure 21 shows the real case size distribution of biomass feedstock. It is reported by Tannous, et al. [66] for milling Douglas Fir in a hammer mill with a screen size of 1.6mm. As discussed, the particles are all mostly much smaller than the given screen size. The highest freqeuency of particles in this distribution are in the 0.32 to 0.64 mm class width. This is also where the average particle size, which was calculated at 0.38 mm, falls. The model framwork developed for normal size disitrubution is implemented to simulate the pyrolsyis of biomass with the irregular size distribution. Figure 22 compares the predictions of heating up time between single and distributed size using Non-isothermal with DEAM. The difference in values highlights the importance of considering the particle size distribution in reactor design of pyrolysis process.

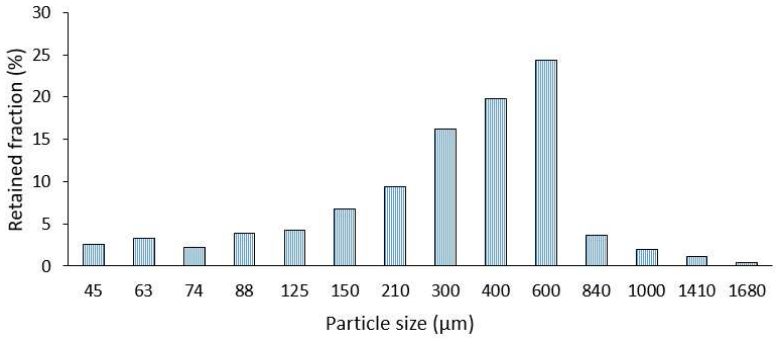

Figure 21 Size distribution of ground biomass from Douglas fir wood analyzed on 14 sieve apertures (data from Tannous, et al., 2012)

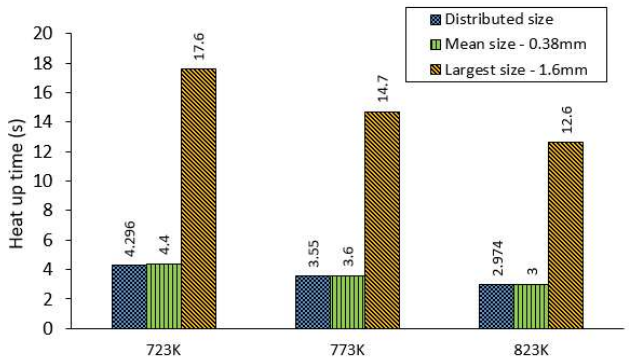

Figure 22 Comparison of heating up time prediction between single and distributed particle size using Non-isothermal with DEAM.

4. Conclusions

To effectively use biomass feedstock with size distribution to produce biofuels, the PBM-DEAM coupled model is first time developed to predict the pyrolysis of biomass particles. The PBM is used to present feedstock population of normal size distribution and irregular size distribution. Two different kinetic models (non-isothermal with/without DAEM), are built into conservation equations of mass and energy. They are compared to demonstrate the prediction performance of size reduction, porosity change and heating-up time during the pyrolysis process of biomass with a size distribution. It is found that

- Non-isothermal kinetics without and with DEAM capture the intra-particle temperature distribution. They are appropriate to predict the heating up time for biomass feedstock with thermally thick particle (Bi>1).
- Particle size of biomass feedstock has a significant impact on heating up time. As the particle diameter increases, so does the time taken for T_c to achieve surrounding temperature.
- There is a noticeable difference of heating-up time between single and distributed particle size.
- For non-isothermal models with and without DEAM, the increase of exposure temperature accelerates heating up of biomass feedstock, particular for thermally thick particle.

The developed model successfully predicted the conversion performance of biomass feedstock with a size distribution. The beneficial outcome will be supportive for the design of pyrolysis reactors and determination of optimal feedstock particle sizes. Further development of the framework is the enhancement of particle habit consideration. In practice, the biomass particles show irregular shapes which have different surface area to volume ratio. This leads to varying conversion performance for different particles. Ultimately, the prediction of real heating-up time of biomass with a size and shape distribution will be calibrated by incorporating transport phenomena thought pore channels and on particle surface coupled with surrounding gas flow.

Acknowledgement

Junmeng Cai appreciated the financial support of this work from CAS Key Laboratory of Renewable Energy (No. Y807k91001). Hongyu Zhu gratefully acknowledges Doctoral Training Programme fund from College of Engineering and Physical Sciences, Aston University.

References:

[1] Mohan D, Pittman CU, Steele PH. Pyrolysis of wood/biomass for bio-oil: A critical review. Energy and Fuels. 2006;20:848-89.
[2] Klinger JL, Westover TL, Emerson RM, Williams CL, Hernandez S, Monson GD, et al. Effect of biomass type, heating rate, and sample size on microwave-enhanced fast pyrolysis product yields and qualities. Applied Energy. 2018;228:535-45.
[3] Dhyani V, Bhaskar T. A comprehensive review on the pyrolysis of lignocellulosic biomass. Renewable Energy. 2018;129:695-716.
[4] Cai J, He Y, Yu X, Banks SW, Yang Y, Zhang X, et al. Review of physicochemical properties and analytical characterization of lignocellulosic biomass. Renewable and Sustainable Energy Reviews. 2017;76:309-22.
[5] Bridgwater AV. Review of fast pyrolysis of biomass and product upgrading. Biomass and Bioenergy. 2012;38:68-94.
[6] Perkins G, Bhaskar T, Konarova M. Process development status of fast pyrolysis technologies for the manufacture of renewable transport fuels from biomass. Renewable and Sustainable Energy Reviews. 2018;90:292-315.
[7] Gao N, Sipra AT, Quan C. Thermogravimetric analysis and pyrolysis product characterization of municipal solid waste using sludge fly ash as additive. Fuel. 2020;281:118572.
[8] Gao N, Kamran K, Quan C, Williams PT. Thermochemical conversion of sewage sludge: A critical review. Progress in Energy and Combustion Science. 2020;79:100843.
[9] Gao N, Jia X, Gao G, Ma Z, Quan C, Naqvi SR. Modeling and simulation of coupled pyrolysis and gasification of oily sludge in a rotary kiln. Fuel. 2020;279:118152.
[10] Chai Y, Wang M, Gao N, Duan Y, Li J. Experimental study on pyrolysis/gasification of biomass and plastics for H2 production under new dual-support catalyst. Chemical Engineering Journal. 2020;396:125260.
[11] Demirbaş A, Arin G. An overview of biomass pyrolysis. Energy Sources. 2002;24:471-82.
[12] Rh Venderbosch WP. Fast pyrolysis technology development. Biofuels. 2010;4:178-208.
[13] Bridgwater AV. Challenges and Opportunities in Fast Pyrolysis of Biomass : Part I. Johnson Matthey Technol Rev. 2018;62:118-30.
[14] Bennadji H, Smith K, Serapiglia MJ, Fisher EM. Effect of particle size on low-temperature pyrolysis of woody biomass. Energy and Fuels. 2014;28:7527-37.
[15] Hounslow MJ. The Population Balance as a Tool for Understanding Particle Rate Processes. KONA Powder and Particle Journal. 1998:179-93.
[16] Hulburt HM, Katz S. Some problems in particle technology: A statistical mechanical formulation. Chemical Engineering Science. 1964;19:555-74.
[17] Abrahamsson PJ, Kvist P, Reynolds G, Yu X, Niklasson Björn I, Hounslow MJ, et al. Analysis of mesoscale effects in high-shear granulation through a computational fluid dynamics–population balance coupled compartment model. Particuology. 2018;36:1-12.
[18] Yu X, Hounslow MJ, Reynolds GK. Representing spray zone with cross flow as a well-

mixed compartment in a high shear granulator. Powder Technology. 2016;297:429-37.
[19] Yu X, Hounslow MJ, Reynolds GK, Rasmuson A, Niklasson Björn I, Abrahamsson PJ. A compartmental CFD-PBM model of high shear wet granulation. AIChE Journal. 2017;63:438-58.
[20] Hounslow MJ, Ryall RL, Marshall VR. A discretized population balance for nucleation, growth, and aggregation. AIChE Journal. 1988;34:1821-32.
[21] Wang B, Mosbach S, Schmutzhard S, Shuai S, Huang Y, Kraft M. Modelling soot formation from wall films in a gasoline direct injection engine using a detailed population balance model. Applied Energy. 2016;163:154-66.
[22] Bellais M, Davidsson KO, Liliedahl T, Sjöström K, Pettersson JBC. Pyrolysis of large wood particles: A study of shrinkage importance in simulations. Fuel. 2003;82:1541-8.
[23] Liu B, Papadikis K, Gu S, Fidalgo B, Longhurst P, Li Z, et al. CFD modelling of particle shrinkage in a fluidized bed for biomass fast pyrolysis with quadrature method of moment. Fuel Process Technol. 2017;164:51-68.
[24] Di Blasi C. Modeling chemical and physical processes of wood and biomass pyrolysis. Progress in Energy and Combustion Science. 2008;34:47-90.
[25] Hough BR, Beck DAC, Schwartz DT, Pfaendtner J. Application of machine learning to pyrolysis reaction networks: Reducing model solution time to enable process optimization. Computers and Chemical Engineering. 2017;104:56-63.
[26] Sharma A, Pareek V, Zhang D. Biomass pyrolysis—A review of modelling, process parameters and catalytic studies. Renewable and Sustainable Energy Reviews. 2015;50:1081-96.
[27] Xiong Q, Yang Y, Xu F, Pan Y, Zhang J, Hong K, et al. Overview of computational fluid dynamics simulation of reactor-scale biomass Pyrolysis. ACS Sustainable Chemistry & Engineering. 2017;5:2783-98.
[28] Burnham AK. Global Chemical Kinetics of Fossil Fuels: How to Model Maturation and Pyrolysis: Springer International Publishing; 2017.
[29] Cai J, Wu W, Liu R. An overview of distributed activation energy model and its application in the pyrolysis of lignocellulosic biomass. Renewable and Sustainable Energy Reviews. 2014;36:236-46.
[30] Li X, Mei Q, Dai X, Ding G. Effect of anaerobic digestion on sequential pyrolysis kinetics of organic solid wastes using thermogravimetric analysis and distributed activation energy model. Bioresour Technol. 2017;227:297-307.
[31] Stankovic B, Jovanovic J, Ostojic S, Adnadjevic B. Kinetic analysis of non-isothermal dehydration of poly(acrylic acid)-g-gelatin hydrogel using distributed activation energy model. Journal of Thermal Analysis and Calorimetry. 2017;129:541-51.
[32] Dong Z, Yang Y, Cai W, He Y, Chai M, Liu B, et al. Theoretical Analysis of Double Logistic Distributed Activation Energy Model for Thermal Decomposition Kinetics of Solid Fuels. Industrial & Engineering Chemistry Research. 2018;57:7817-25.
[33] Cai J, Liu R. New distributed activation energy model: Numerical solution and application to pyrolysis kinetics of some types of biomass. Bioresour Technol. 2008;99:2795-9.
[34] Cai J, Wu W, Liu R, Huber GW. A distributed activation energy model for the pyrolysis of lignocellulosic biomass. Green Chemistry. 2013;15:1331-40.
[35] Kolditz O. Finite Volume Method. In: Kolditz O, editor. Computational Methods in Environmental Fluid Mechanics. Berlin, Heidelberg: Springer Berlin Heidelberg; 2002. p. 173-90.
[36] Li J, Paul MC, Younger PL, Watson I, Hossain M, Welch S. Characterization of biomass combustion at high temperatures based on an upgraded single particle model. Appl Energy. 2015;156:749-55.
[37] Di Blasi C. Heat, momentum and mass transport through a shrinking biomass particle

exposed to thermal radiation. Chemical Engineering Science. 1996;51:1121-32.
[38] Yang YB, Sharifi VN, Swithenbank J, Ma L, I L, Jones JM, et al. Combustion of a Single Particle of Biomass. Energy. 2008:306-16.
[39] Li J, Paul MC, Younger PL, Watson I, Hossain M, Welch S. Prediction of high-temperature rapid combustion behaviour of woody biomass particles. Fuel. 2016;165:205-14.
[40] Grieco E, Baldi G. Analysis and modelling of wood pyrolysis. Chemical Engineering Science. 2011;66:650-60.
[41] Koufopanos CA, Papayannakos N, Maschio G, Lucchesi A. Modelling of the pyrolysis of biomass particles. Studies on kinetics, thermal and heat transfer effects. The Canadian Journal of Chemical Engineering. 1991;69:907-15.
[42] Huang QX, Wang RP, Li WJ, Tang YJ, Chi Y, Yan JH. Modeling and Experimental Studies of the Effects of Volume Shrinkage on the Pyrolysis of Waste Wood Sphere. Energy & Fuels. 2014;28:6398-406.
[43] Chan W-CR, Kelbon M, Krieger BB. Modelling and experimental verification of physical and chemical processes during pyrolysis of a large biomass particle. Fuel. 1985;64:1505-13.
[44] Galgano A, Blasi CD. Modeling Wood Degradation by the Unreacted-Core-Shrinking Approximation. Industrial & Engineering Chemistry Research. 2003;42:2101-11.
[45] Porteiro J, Granada E, Collazo J, Patiño D, Morán JC. A Model for the Combustion of Large Particles of Densified Wood. Energy & Fuels. 2007;21:3151-9.
[46] Park WC, Atreya A, Baum H. Experimental and theoretical investigation of heat and mass transfer processes during wood pyrolysis2010.
[47] Bharadwaj A, Baxter LL, Robinson AL. Effects of intraparticle heat and mass transfer on biomass devolatilization: Experimental results and model predictions. Energy and Fuels. 2004;18:1021-31.
[48] Johansen JM, Jensen PA, Glarborg P, Mancini M, Weber R, Mitchell RE. Extension of apparent devolatilization kinetics from thermally thin to thermally thick particles in zero dimensions for woody biomass. Energy. 2016;95:279-90.
[49] Lu H, Robert W, Peirce G, Ripa B, Baxter LL. Comprehensive study of biomass particle combustion. Energy and Fuels. 2008;22:2826-39.
[50] Luo H, Wu H, Lin W, Dam-Johansen K, Luo H. Heat transfer corrected isothermal model for devolatilization of thermally-thick biomass particles. 2017.
[51] Pyle DL, Zaror CA. Heat transfer and kinetics in the low temperature pyrolysis of solids. Chemical Engineering Science. 1984;39:147-58.
[52] Yu X, Hounslow MJ, Reynolds GK. Accuracy and optimal sampling in Monte Carlo solution of population balance equations. 2015;61:2394-402.
[53] Yu X, Hassan M, Ocone R, Makkawi Y. A CFD study of biomass pyrolysis in a downer reactor equipped with a novel gas–solid separator-II thermochemical performance and products. Fuel Processing Technology. 2015;133:51-63.
[54] Bhavanam A, Sastry RC. Kinetic study of solid waste pyrolysis using distributed activation energy model. Bioresour Technol. 2015;178:126-31.
[55] Burnham AK. Global kinetic analysis of complex materials. Energy Fuels. 1999;13:1-22.
[56] Cai J, Jin C, Yang S, Chen Y. Logistic distributed activation energy model – Part 1: Derivation and numerical parametric study. Bioresour Technol. 2011;102:1556-61.
[57] Sadhukhan AK, Gupta P, Saha RK. Modelling of pyrolysis of large wood particles. Bioresour Technol. 2009;100:3134-9.
[58] Paulauskas R, Džiugys A, Striugas N. Experimental investigation of wood pellet swelling and shrinking during pyrolysis. Fuel. 2015;142:145-51.
[59] Rezaei H, Sokhansanj S, Bi X, Lim CJ, Lau A. A numerical and experimental study on fast pyrolysis of single woody biomass particles. Appl Energy. 2017;198:320-31.
[60] Cai J, Xu D, Dong Z, Yu X, Yang Y, Banks SW, et al. Processing thermogravimetric

analysis data for isoconversional kinetic analysis of lignocellulosic biomass pyrolysis: Case study of corn stalk. Renewable and Sustainable Energy Reviews. 2018;82:2705-15.
[61] Luo H, Wu H, Lin W, Dam-Johansen K. Heat transfer corrected isothermal model for devolatilization of thermally-thick biomass particles. Stockholm: Technical University of Denmark; 2017.
[62] Gauthier G, Melkior T, Salvador S, Corbetta M, Frassoldati A, Pierucci S, et al. Pyrolysis of Thick Biomass Particles: Experimental and Kinetic Modelling. Chemical Engineering Transactions. 2013;23:601-6.
[63] Papadikis K, Gu S, Bridgwater AV, Gerhauser H. Application of CFD to model fast pyrolysis of biomass. Fuel Processing Technology. 2009;90:504-12.
[64] Bennadji H, Smith K, Serapiglia MJ, Fisher EM. Effect of Particle Size on Low-Temperature Pyrolysis of Woody Biomass. Energy & Fuels. 2014;28:7527-37.
[65] Wiggins GM, Ciesielski PN, Daw CS. Low-Order Modeling of Internal Heat Transfer in Biomass Particle Pyrolysis. Energy & Fuels. 2016;30:4960-9.
[66] Tannous K, Lam PS, Sokhansanj S, Grace JR. Physical properties for flow characterization of ground biomass from douglas fir wood. Particulate Science and Technology. 2013;31:291-300.